A NEW FRAMEWORK FOR AUTOMATED IDENTIFICATION OF PATHOLOGICAL TISSUES IN CONTRAST ENHANCED CARDIAC MAGNETIC RESONANCE IMAGES

Ahmed Elnakib[1], *Garth M. Beache*[2], *M. Nitzken*[1], *Georgy Gimel'farb*[3], *and Ayman El-Baz*[1*]

[1] BioImaging Laboratory, Bioengineering Department, University of Louisville, Louisville, KY, USA.
[2] Department of Diagnostic Radiology, School of Medicine, University of Louisville, Louisville, KY, USA.
[3] Department of Computer Science, University of Auckland, Auckland, New Zealand.

ABSTRACT

A novel automated framework for quantification of myocardial viability in contrast enhanced cardiac magnetic resonance images (CE-CMRI) is proposed. The framework consists of three main steps. First, the inner and outer borders of the left ventricle (LV) wall (myocardium wall) are segmented from the surrounding tissue. Second, the pathological tissue in the myocardium wall is identified using a MAP-based classifier based on the visual appearance and spatial interaction of the LV pathological tissue as well as healthy tissue. Third, the myocardial viability is assessed and quantified based on measuring two parameters: the percentage of pathological tissue with respect to the area of the myocardium wall and the transmural extent of the pathological tissue in the myocardium wall. The transmural extent is estimated based on a new Partial Differential Equation (PDE) approach to determine point-to-point correspondences between the inner and outer borders of the pathological area as well as the myocardium wall. The proposed framework was tested on *in-vivo* CE-CMR images and validated with manual expert delineations of pathological tissue. Experiments and comparison results on real CE-CMR images confirm the robustness and accuracy of the proposed framework over the existing ones.

Index Terms— Myocardial Viability, Left Ventricle, Segmentation, Contrast Enhanced Cardiac Magnetic Resonance Images.

1. INTRODUCTION

Assessment of myocardial viability by identifying pathological tissue in the myocardium is of great importance. Clinically, it is the standard way for diagnosing ischemic heart disease and LV dysfunction as well as for guiding optimized therapies for individual patients [1].

To reliably assess the pathological tissue, one has to accurately segment the pathological tissue from the LV wall. The segmentation of the pathological tissue is a challenge due to possible image noise, poor resolution, or diffuse boundaries. Manual outlining of the pathological tissue enables the area of the pathological tissue to be determined. However, it is tedious and time consuming. Automated or semi-automated myocardial viability assessment techniques overcome this drawback. Most of these techniques use empirical simple intensity-thresholding estimates to identify the pathological tissue. The commonly used estimates for pathological tissue's intensities are those of more than two [2] or three [3] standard deviations (σ) above the average intensity of a remote healthy myocardial region. To enhance the thresholded extracted regions, Heiberg et al. [4] used level-set regulation. Hennemuth et al. [5] analyzed the image intensity profile to initiate a watershed-based segmentation. Recently, Elagouni et al. [6] used fuzzy thresholding followed by region analysis.

Based on the identified pathological tissue, two important parameters can be estimated to quantify the myocardium viability: the percentage of the pathological tissue with respect to the area of the myocardium wall, and the transmural extent of the pathological tissue in the LV wall. The traditional procedure (e.g., used in [7, 8]) to estimate the transmural extent is based on extending a fixed number of radial lines from the inner to the outer contour of the LV (see Fig. 1(a)). The portion of pathological tissue in each line is computed, and the transmural extent is estimated as the average of the pathological tissue's extent in these lines. This procedure leads to inaccurate estimation of point-to-point correspondence and inconsistency in the estimation of the transmural extent.

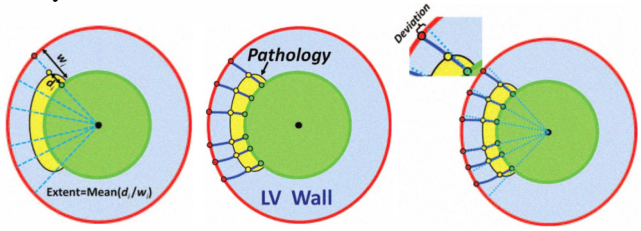

(a) (b) (c)

Fig. 1. Illustration of estimating the transmural extent of pathological tissue in the LV wall: (a) traditional approach, (b) proposed approach, and (c) deviations of (a) from the co-located corresponding pixel pairs of (b).

The aforementioned assessment techniques have the following limitations: (*i*) the pathology segmentation approaches did not take into account the spatial interaction between the myocardium pixels, (*ii*) most of them suffer from sensitivity to imperfect myocardium contours and are subjected to errors in noisy images, and (*iii*) the traditional procedure for transmural extent estimation suffers from inconsistency in estimating the point-to-point correspondence. To overcome these limitations, we propose an automatic framework to analyze CE-CMR images. The proposed framework identifies the pathological tissue in the myocardium wall based on a joint Markov-Gibbs Random Field (MGRF) model that accounts for both the 1st-order visual appearance of the segmented myocardium wall as well as the spatial interaction between its pixels. The transmural extent is estimated using a partial differential equation (PDE)-based approach to accurately co-locate the corresponding pixel pairs between the inner and outer contours of the LV and between the inner and outer edges of the pathological tissue's area as shown in Fig. 1(b). This approach overcomes the inconsistency and deviations of the traditional procedure as shown in Fig. 1(c).

* Corresponding Author:- Tel: (502) 852-5092, Fax: (502) 852-6806, E-mail: aselba01@louisville.edu

2. BASIC ANALYSIS STAGES

We propose a new framework for automated quantification of myocardial viability in CE-CMRI (see Fig. 2). In this paper, we will focus on steps 2 and 3 and step 1 is shown in detail in [9].

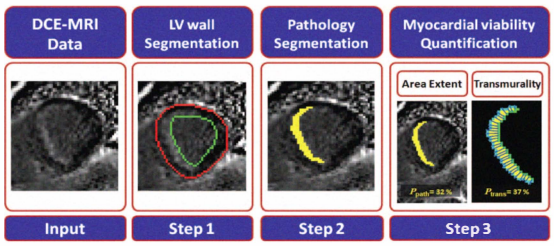

Fig. 2. The proposed framework for analyzing CE-CMR images

2.1. Segmentation of the pathological tissue in the LV wall

The segmentation of the pathological tissue of the LV is a challenging task. This stage proposes a powerful approach for pathological tissue segmentation based on an identifiable joint Markov-Gibbs Random Field (MGRF) model of CE-CMRI and "object–background" region maps.

2.1.1. Joint MGRF model of the pathological tissue and background

Let $\mathbf{Q} = \{0, \ldots, Q-1\}$, and $\mathbf{L} = \{\text{ob}, \text{bg}\}$ be a set of Q integer gray levels, and a set of object ("ob") and background ("bg") labels. Let a 2D arithmetic grid $\mathbf{R} = \{(x, y) : x = 0, 1, \ldots, X-1; y = 0, 1, \ldots, Y-1\}$ support grayscale CE-CMRI $\mathbf{g} : \mathbf{R} \to \mathbf{Q}$, their binary region maps $\mathbf{m} : \mathbf{R} \to \mathbf{L}$. The CE-CMRI and their region maps $\mathbf{m}$ are modeled with a joint MGRF model as follows:

$$P(\mathbf{g}, \mathbf{m}) = P(\mathbf{g}|\mathbf{m})P(\mathbf{m}) \tag{1}$$

combining a 2nd-order MGRF $P(\mathbf{m})$ of region labels for a spatially homogeneous evolving region map $\mathbf{m}$ and a 1st-order conditionally independent random field $P(\mathbf{g}|\mathbf{m})$ of image intensities given the map.

We focus on accurate identification of spatial interactions in $P(\mathbf{m})$, and pixel-wise distributions of intensities in $P(\mathbf{g}|\mathbf{m})$. To perform the initial pathological tissue segmentation, the conditional image intensity model $P(\mathbf{g}|\mathbf{m})$ is used to build an initial region map. The final segmentation is performed by optimizing the identified joint MGRF model of the CE-CMRI and region maps using stochastic relaxation.

2.1.2. Spatial interaction in the LV wall

For a more accurate segmentation, spatially homogeneous interactions between the region labels are modeled with the popular Potts model (the MGRF with the nearest 8-neighborhood) having bi-valued Gibbs potentials, depending only on whether the nearest pairs of labels are equal or not.

The 8-neighborhood, $\mathbf{N}_a$, has two types of symmetric pairwise interactions specified by the absolute distance $a \in \mathbf{A} = \{1, \sqrt{2}\}$ between two pixels in the same and adjacent MRI slices: (*i*) the closest pairs with the inter-pixel coordinate offsets $\mathbf{N}_1 = \{(\pm 1, 0), (0, \pm 1)\}$; and (*ii*) the farther diagonal pairs with the offsets $\mathbf{N}_{\sqrt{2}} = \{(1, \pm 1), (-1, \pm 1)\}$. To identify the MGRF model, approximate analytical maximum likelihood estimate of the 3D Gibbs potentials, $V_{a,\text{eq}}, V_{a,\text{ne}}$ are derived in line with [10]: $V_{a,\text{eq}} = -V_{a,\text{ne}} = 2\,(f_{\text{eq}}(\mathbf{m}) - 1/2)$; where $f_{a,\text{eq}}(\mathbf{m})$ denotes the relative frequency of the equal label pairs in the equivalent pixel pairs $\{((x, y), (x+\xi, y+\eta)) : (x, y) \in \mathbf{R};\ (x+\xi, y+\eta) \in \mathbf{R};\ (\xi, \eta) \in \mathbf{N}_a\}$.

2.1.3. Conditional intensity model for CE-CMRI slice

Just as in [11], an MRI, given a region map, is modeled with a simple conditionally independent random field of pixel intensities:

$$P(\mathbf{g}|\mathbf{m}) = \prod_{(x,y,z) \in \mathbf{R}} p_{m_{x,y,z}}(\mathbf{g}_{x,y,z})$$

where the pixel-wise probability distributions $p_\lambda = [p_\lambda(q) : q \in \mathbf{Q}]$; $\lambda \in \mathbf{L}$, for the pathological tissue and its background are estimated during the segmentation. To separate p_0 and p_1, the mixed empirical distribution of all pixel intensities is closely approximated with a linear combination of discrete Gaussians (LCDG) with two dominant modes related to the object (i.e. the pathological tissue) and background, respectively. The LCDG including numbers of its positive and negative terms is obtained with our previous Expectation-Maximization-based algorithm introduced in [11].

2.1.4. Segmentation Algorithm

To accurately identify the pathological tissue in the LV wall, we used a MAP-based classification approach that accounts for intensity and spatial interactions between the pixels of the myocardium wall as follows:

1. Estimate the marginal density of the pathological tissue in the extracted myocardium wall from each CE-CMR image (1st-order visual appearance) using the modified EM algorithm with linear combinations of discrete Gaussians (LCDG) [11].
2. Use the estimated intensity model to get the initial segmentation of the pathological tissue, i.e., form an initial region map of pathological tissue.
3. Use stochastic relaxation (Iterative Conditional Mode (ICM) [12]) algorithm to estimate the final map (segmentation of pathological tissue) that maximizes the joint MGRF model.

2.2. Myocardial viability quantification

After accurately segmenting the pathological tissue, two potential myocardial viability quantification parameters have been derived. Namely, the percentage of pathological tissue and the transmural extent of the pathological tissue (the transmurality). Such parameters allow for both diagnosis and therapy guidance for LV dysfunction and ischemic heart diseases.

2.2.1. Percentage of pathological tissue

To estimate the percentage of pathological tissue (P_{path}), we divide the detected area of pathological tissue by the total area of the myocardium wall (as shown in Fig 3):

$$P_{\text{path}} = \frac{\text{Area of pathological tissue } (A_1)}{\text{Total area of myocardium wall } (A_2)} \times 100\% \tag{2}$$

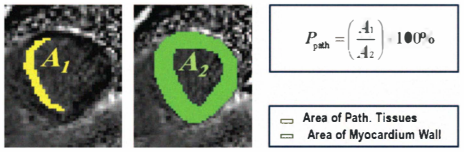

Fig. 3. Estimation of the percentage of the pathological tissue.

2.2.2. *The transmural extent of the pathological tissue*

The transmural extent of the pathological tissue (transmurality), an important parameter for therapy decisions, is defined as the degree of penetration of the pathological tissue in the myocardium wall [17]. The traditional estimation procedure for the transmural extent leads to inaccurate estimation of point-to-point correspondence and inconsistency in the estimation of the transmural extent as illustrated in Section 1. In this paper, we propose a partial differential equation (PDE)-based approach to co-locate the corresponding pixel pairs between the inner and outer contours of the LV and between the inner and outer edges of the pathological tissue's area as shown in Fig. 4. The correspondences, or matches between the borders' points, are found by solving the partial differential Laplace equation for a scalar potential field γ [18].

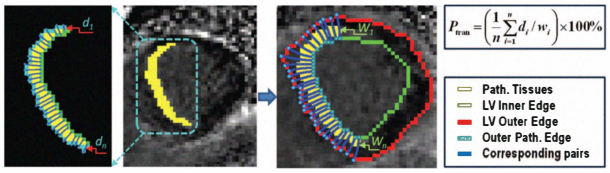

Fig. 4. Step by step illustration of the transmural extent estimation: detecting the pathological tissue in the LV wall (middle), and estimating the wall thickness w (right) and the pathological extent d (left) in the detected region.

Laplace's equation is a 2nd-order linear partial differential equation (PDE) for a scalar field. It arises in a variety of applications including fluid mechanics, electromagnetism, potential theory, solid mechanics, heat conduction, geometry, probability, etc. Mathematically, the planer Laplace equation takes the following form:

$$\nabla^2 \gamma = \frac{\partial^2 \gamma}{\partial^2 x^2} + \frac{\partial^2 \gamma}{\partial^2 y^2} = 0 \qquad (3)$$

Generally, the solution of the Laplace equation between two boundaries, such as P_A and P_B in Fig. 5, results in intermediate equipotential surfaces (dashed lines in Fig. 5) and streamlines that connect both the boundaries. The streamlines (e.g., the line connecting the points P_{ai} and P_{bj} in Fig. 5) are orthogonal to all the equipotential surfaces and establish the point-to-point correspondences between the boundaries. To estimate the transmural extent, the correspondence between the inner and outer borders of the pathological tissue's area and of the LV wall are found by solving the Laplace equation (see Fig. 4). The transmural extent is the average ratio between the pathological extent d and the wall thickness w, and it is estimated as follows:

$$P_{\text{trans}} = \left(\frac{1}{n}\sum_{i=1}^{n}\frac{d_i}{w_i}\right) \times 100\% \qquad (4)$$

where n is the number of lines that connect the corresponding pairs estimated by solving the Laplace equation.

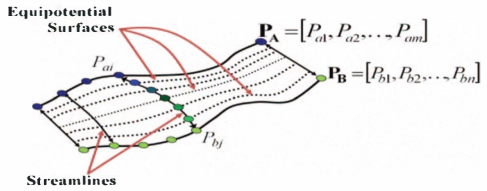

Fig. 5. 2D correspondences by a potential field.

3. EXPERIMENTAL RESULTS

The proposed framework has been tested on seven data sets of 2D CE-CMR images, each consisting of 11 image cross sections over the left ventricle (total of 77 images). The images were delayed-contrast agent acquisitions, using a phase sensitive inversion recovery technique, of typical spatial resolution 2.08 × 2.08 × 8.0 mm^3. All the images are acquired using a Siemens 1.5T system with multichannel phased array reception coils [19]. To evaluate the segmentation accuracy of the proposed framework, the "ground truth" delineations of the pathological tissue in each image were given by an expert (radiologist).

To assess the myocardium viability, we first identify the pathological tissue. Fig. 6 illustrates the results of the proposed approach for pathological tissue identification compared with the manual ground truth expert delineation. To quantify the myocardial viability, we use two key parameters: the percentage of pathological tissue and the transmural extent. Fig. 6 and Fig. 7 demonstrate the estimated percentage of pathological tissue and the transmural extent for typical image cases. Table. 1 shows the results of the estimated percentage of pathological tissue in comparison to the ground truth expert delineations and two standard pathological segmentation approaches, namely the 2σ [2] and 3σ [3] techniques. As demonstrated in Table. 1, the difference in the mean percentage of pathological tissue between the ground truth expert delineation and the proposed segmentation is not statistically significant according to the unpaired t-test (the two-tailed P value is less than or equal to 0.2762), while it is statistically significant between the ground truth and the 2σ and 3σ techniques, respectively. To highlight that the proposed approach can be used to monitor the post-treatment of patients, Table. 2 shows the two extracted parameters for myocardium viability quantification for one patient over one year of treatment using the standard 17-segment model [20] illustrated in Fig. 8.

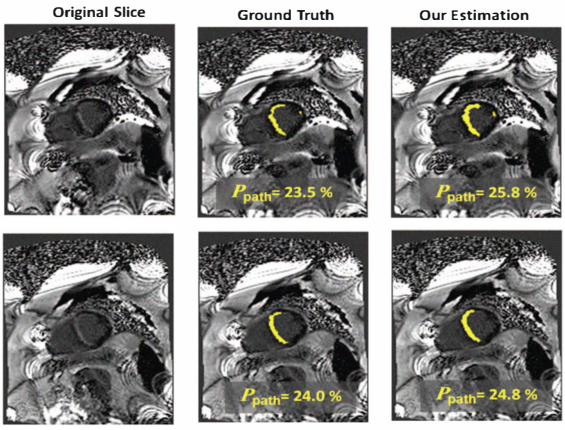

Fig. 6. Results of our proposed pathological tissue identification approach compared with the manual ground truth expert delineation: P_{path} denotes the percentage of the pathological tissue in the myocardial segmented wall.

Table 1. Results of the estimated percentage of pathological tissue in comparison to the ground truth expert delineations and two standard pathological segmentation approaches, namely the 2σ and 3σ techniques.

	GT	Our	2σ [2]	3σ [3]
Minimum P_{path}, %	0.0	0.0	2.7	0
Maximum P_{path},%	43.3	26.8	19.0	7.3
Mean P_{path}, %	17.7	14.1	8.4	1.1
Std. dev.,%	12.51	9.27	5.12	1.97
P-value		0.2762	0.0019	$\leq 10^{-4}$

Table 2. The two extracted parameters for myocardium viability quantification (i.e., $P_{\texttt{path}}$ and $P_{\texttt{trans}}$) for one patient over one year of treatment.

Section Number		1	2	3	4	5	6	7	8	9	10	11	12	13	14	15	16	17	Mean
$P_{\texttt{path}}$, %	Pre	4.6	2.8	22.0	21.4	12.7	0.0	0.0	0.0	13.1	31.7	1.2	0.0	0.0	0.0	1.8	0.0	0.0	**6.5**
	Post	0.0	0.0	17.8	18.0	4.6	0.0	0.0	0.0	0.91	19.2	2.1	0.0	0.0	0.0	0.9	0.0	0.0	**2.1**
$P_{\texttt{trans}}$, %	Pre	3.1	0.7	7.7	19.6	10.4	0.0	0.0	0.0	13.8	31.5	1.2	0.0	0.0	0.0	1.1	0.0	0.0	**5.3**
	Post	0.0	0.0	7.2	0.0	0.0	0.0	0.0	0.0	0.0	12.4	1.6	0.0	0.0	0.0	0.3	0.0	0.0	**1.3**

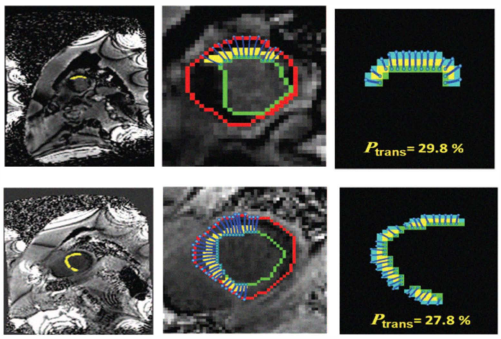

Fig. 7. The estimated percentage of transmural extent $P_{\texttt{trans}}$ on two typical image cases.

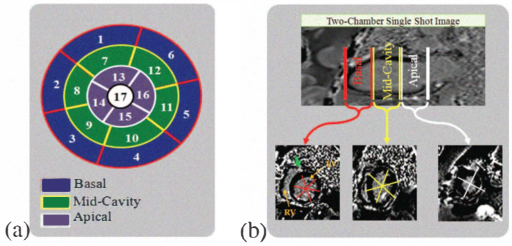

Fig. 8. The myocardial 17-segment model [20]: (a) circumferential polar plot and (b) locations of segments for basel (left), mid-cavity (middle), and apical (right) image sections. The segment numbering starts contour-clockwise from the anatomical landmark indicated by the green arrow in the basal section.

4. CONCLUSION

A fully-automated framework for quantification of myocardial viability is proposed. The framework presents a powerful approach for segmenting the pathological tissue from CE-CMR images. The approach takes into account the spatial interaction between the myocardium pixels to ensure the homogeneity of the segmented tissue. In addition, the proposed framework provides a new method to accurately estimate the transmural extent of the pathological tissues in the LV wall and overcome the inconsistencies of the traditional estimation method. The estimated myocardial viability quantification parameters allow for both diagnosis and therapy planning. Experiments with CE-CMR images and manually segmented expert delineations confirm the robustness and the accuracy of the proposed approach. In our future work, we plan to extend the proposed 2D framework to include 3D cardiac objects to quantitatively characterize the effectiveness and robustness of the proposed scheme.

5. REFERENCES

[1] H. P. Kühl, et al., "Myocardial viability in chronic ischemic heart disease: comparison of contrast-enhanced magnetic resonance imaging with (18)F-fluorodeoxyglucose positron emission tomography," *J Am Coll Cardiol,* pp. 1341–1348, 2003.

[2] R. J. Kim, et al., "Relationship of MRI delayed contrast enhancement to irreversible injury, infarct age, and contractile function," *Circulation,* vol. 100, pp. 1992–2002, 1999.

[3] D. S. Fieno, et al., "Contrast-enhanced magnetic resonance imaging of myocardium at risk: distinction between reversible and irreversible injury throughout infarct healing," *J Am Coll Cardiol,* vol. 36, no. 6, pp. 1985–1991, 2000.

[4] E. Heiberg, et al., 'Semi-automatic quanti..cation of myocardial infarction from delayed contrast enhanced magnetic resonance imaging," *Scandinavian Cardiovascular J.,* 2005.

[5] A. Hennemuth, et al., "A comprehensive approach to the analysis of contrast enhanced cardiac MR images," *IEEE TMI,* 2008.

[6] K. Elagouni, et al., "Automatic segmentation of pathological tissues in cardiac MRI," *ISBI'10,* pp. 472–475, 2010.

[7] N. Noble, et al., "The automatic identification of hibernating myocardium," *MICCAI'04,* 2004, pp. 890–898.

[8] S. Nazarian, et al., "Magnetic resonance assessment of the substrate for inducible ventricular tachycardia in nonischemic cardiomyopathy," *Circulation,* vol. 112, pp. 2821-2825, 2005.

[9] A. Elnakib, et al., "A new framework for automated segmentation of left ventricle wall from cardiac magnetic resonance images," *submitted to ICIP 2011.*

[10] A. Farag, A. El-Baz, and G. Gimel'farb, "Precise segmentation of multimodal images," *IEEE Transactions on Image Processing,* vol. 15, no. 4, pp. 952–968, 2006.

[11] A. El-Baz and G. Gimel'farb, "EM Based approximation of empirical distributions with linear combinations of discrete Gaussians," in *Proc. of IEEE Int. Conf. on Image Processing (ICIP'07), San Antonio, Texas, USA,* September 16–19, 2007, vol. 4, pp. 373–376.

[12] J. Besag, "On the statistical analysis of dirty pictures," *Journal of the Royal Statistical Society. Series B*, pp. 259–302, 1986.

[13] L. R. Dice, "Measures of the Amount of Ecologic Association Between Species," *Ecological society of America,* 1945.

[14] P. Viola and W. M. Wells, "Alignment by maximization of mutual information," *ICCV'95,* 1995, pp. 16–23.

[15] L. Cohen and R. Kimmel, "Global minimum for active contour models: A minimal path approach," *Int. J. Computer Vision,* 1997.

[16] D. Adalsteinsson and J. Sethian, "A fast level set method for propagating interfaces," *J. Computational Physics,* 1995.

[17] K. Choi, et al., "Transmural extent of acute myocardial infarction predicts long-term improvement in contractile function," *Circulation,* vol. 104, no. 10, pp. 1101-1107, 2001.

[18] S. Jones, et al., "Three-dimensional mapping of cortical thickness using Laplace's equation," *Human Brain Mapping,* 2000.

[19] R. J. Kim, et al., "How we perform delayed enhancement imaging," *Journal of Cardiovascular MR,* pp. 505–514, 2003.

[20] M. Cerqueira, , et al., "Standardized myocardial segmentation and nomenclature for tomographic imaging of the heart," *Circulation,* vol. 105, pp. 539–542, 2002.